


ORIGINAL ARTICLE

Open Access



Indeterminate Domain Proteins Regulate Rice Defense to Sheath Blight Disease

Qian Sun^{1†}, Dan Dan Li^{1†}, Jin Chu^{2†}, De Peng Yuan¹, Shuang Li^{3,4}, Li Juan Zhong⁵, Xiao Han^{6*} and Yuan Hu Xuan^{1*} 

Abstract

Background: Loose Plant Architecture 1 (LPA1), an indeterminate domain (IDD) protein, exhibits almost no expression in the leaves, but the overexpression of *LPA1* significantly increases the resistance of rice to sheath blight disease (ShB) via the activation of *PIN-FORMED 1a* (*PIN1a*).

Results: In this study, we determined that *Rhizoctonia solani* infection significantly induced *LPA1* expression in the leaves, and *lpa1* was more susceptible to *R. solani* compared with the wild-type and revertant plants. In addition, infection with *R. solani* altered the expression of *IDD3*, *IDD5*, *IDD10*, and *IDD13*, and yeast two-hybrid, split-GFP, and coimmunoprecipitation assays showed that LPA1 interacts with *IDD3* and *IDD13*. *IDD13 RNAi* plants were more susceptible, while *IDD13* overexpressors were less susceptible to ShB compared with the wild-type. In parallel, *idd3* exhibited no significant differences, while *IDD3* overexpressors were more susceptible compared to the wild-type response to ShB. Additional chromatin-immunoprecipitation and electrophoretic mobility shift assay experiments indicated that *IDD13* and *IDD3* bound to the *PIN1a* promoter, and the transient assay indicated that *IDD13* and *IDD3* positively and negatively regulate *PIN1a* expression, respectively. Moreover, *IDD13*, *IDD3*, and *LPA1* form a transcription factor complex that regulates *PIN1a*. A genetic study showed that the *LPA1* repressor lines were similar to *lpa1/IDD13 RNAi* and were more susceptible than the *lpa1* and *IDD13 RNAi* plants in response to ShB. The overexpression of *IDD13* increased resistance to ShB in the *lpa1* background.

Conclusions: Taken together, our analyses established that *IDD3*, *IDD13*, and *LPA1* form a transcription factor complex to regulate the defense of rice against ShB possibly via the regulation of *PIN1a*.

Keywords: Indeterminate domain protein, Sheath blight disease, Transcription activation, Defense, Rice

Background

Sheath blight disease (ShB) is one of the three major diseases that are caused by *Rhizoctonia solani* in rice (*Oryza sativa*) (Savary et al., 1995). The fungus damages rice during the whole period of the growth cycle and primarily infects the leaves, sheaths, and panicles. At the late stage of infection, the whole plant withers and lodges (Savary et al., 1995). ShB can reduce rice yield production up to 50% when the disease is severe (Savary et al. 2000). Since there is a lack of resistant cultivars against ShB, the application of fungicides is the current

primary approach to control this disease (Savary et al. 2000). However, its use severely influences environmental conditions because of its effect on microbes in the environment, and the fungicides also increase the cost of cultivation. Thus, the isolation of resistant rice cultivars and the exploration of defense mechanisms against ShB have become an important issue. Previous studies have demonstrated that the overexpression of chitinase, β -1,3-glucanase, or polygalacturonase-inhibiting protein (OsP-GIP1) enhances the resistance of rice to *R. solani* (Shah et al. 2009; Mao et al. 2014; Wang et al. 2015). The overexpression of an ethylene synthesis enzyme (OsACS2) promotes the resistance of rice to blast and sheath blight (Helliwell et al. 2013). The overexpression of BROAD-SPECTRUM RESISTANCE2 (BSR2) resulted in resistance to *R. solani* in Arabidopsis and rice (Maeda et al. 2019), and salicylic acid-dependent immunity contributes to resistance against *R. solani* in rice and *Brachypodium*

* Correspondence: xiaohan@caas.cn; xuanyuanhu115@syau.edu.cn

[†]Qian Sun, Dan Dan Li and Jin Chu contributed equally to this work.

⁶College of Biological Science and Engineering, Fuzhou University, Fuzhou 350108, China

¹College of Plant Protection, Shenyang Agricultural University, Shenyang 110866, China

Full list of author information is available at the end of the article

distachyon (Kouzai et al. 2018). In addition, our recent studies identified that a mutation in *Sugar Will be Eventually be Exported Transporter 11* (*SWEET11*) significantly promoted the defense of rice to ShB (Gao et al. 2018); Related to ABI3/VP1-Like 1 (RAVL1) modulates rice defense against ShB via the activation of brassinosteroids and ethylene signaling genes (Yuan et al. 2018), and the overexpression of *LPA1* (*IDD14*) promoted the defense of rice against ShB via the activation of *PIN1a* (Sun et al. 2019).

The indeterminate domain (IDD) consists of two C₂H₂ and two C₂HC zinc finger motifs, and the IDD genes play diverse biological functions in plants. ID1 has been reported to control the flowering time in maize and rice (Colasanti et al. 1998; Park et al. 2008). Magpie (MAG)/AtIDD3 and jackdaw (JKD)/AtIDD10 regulate the fate of root cells (Welch et al. 2007). Enhydrous (ENY)/AtIDD1 regulates seed maturation (Feurtado et al. 2011). AtIDD8 modulates plant development (Seo et al. 2011). AtIDD14, AtIDD15, and AtIDD16 cooperatively regulate lateral organ morphogenesis and gravitropism by promoting auxin biosynthesis and transport in Arabidopsis (Cui et al. 2013). Loose plant architecture1 (*LPA1*)/IDD14 regulates shoot gravitropism and lamina joint angle (Wu et al. 2013; Liu et al. 2016). The regulator of CBF1 (ROC1)/IDD3 activates DREB1B/CBF1 to regulate chilling tolerance in rice (Dou et al. 2016). IDD2 regulates secondary cell wall formation in rice (Huang et al. 2018). In addition, the AtIDD4 repressor constitutively induces immunity in Arabidopsis (Volz et al. 2019). The binding motifs of the transcription factor IDD have been identified in maize (ID1, 5'-TTTGTC^G/C'TTTT-3'), Arabidopsis (AtIDD8, 5'-TTTTGTCC-3'), and rice (IDD10, 5'-TTTGTC^C/C) (Kozaki et al. 2004; Seo et al. 2011; Xuan et al. 2013). However, the function of IDD in plant defense, as well as the IDD target genes, remains largely unknown.

Auxin is one of the key phytohormones, and its polar transport is regulated by auxin influx AUX1/LAX and efflux protein PINs (Adamowski and Friml, 2015; Zazimalova et al. 2010). Auxin plays key roles in plant growth and development, as well as in controlling plant defense (Robert-Seilaniantz et al. 2011; Naseem et al. 2012; Chen et al. 2007). More studies identified that auxin signaling regulates rice defense against the bacterial pathogen *Xanthomonas oryzae* (Fu et al. 2011) and the fungal pathogen *Magnaporthe oryzae* (Fu et al. 2011). Recently, we identified that exogenously treated auxin increases the resistance of rice to *R. solani* AG1-IA and revealed that *LPA1* overexpression activates *PIN1a* to promote defense against *R. solani* in rice (Sun et al. 2019). However, whether other IDDs regulate the resistance of rice to ShB remains to be elucidated. In this study, we performed molecular, biochemical, and genetic studies to explore the function of IDD in rice defense. The results showed that IDD3 and IDD13 interact with *LPA1* to regulate *PIN1a* expression and act to modulate the resistance of rice

to ShB. Taken together, our analyses provide information on the role of the IDDs in the regulation of rice defense, as well as the regulatory mechanism for ShB in rice.

Results

LPA1 Is Induced by *Rhizoctonia solani*, and *lpa1* Is more Susceptible to Sheath Blight Disease

Previously we demonstrated that the overexpression of *LPA1* significantly promotes the resistance of rice to ShB via the activation of *PIN1a* (Sun et al. 2019). However, previous research indicated that *LPA1* was expressed at very low levels in the leaves and sheath (Wu et al. 2013). Therefore, we analyzed the *R. solani* infection-dependent *LPA1* expression in more detail. Interestingly, infection with *R. solani* significantly induced *LPA1* expression after 72 h (Fig. 1a). Examination of the response of *lpa1*, *LPA1* revertant (Rev.), and wild-type (WT) plants (Liu et al. 2016) showed that *lpa1* was more susceptible to *R. solani* AG1-IA than the WT and revertant (Rev.) plants (Fig. 1b). The percentage of the leaf area covered with lesions was 41% in the WT, 56% in *lpa1*, and 39% in Rev. (Fig. 1c). Since *LPA1* activates *PIN1a* transcription, the *PIN1a* expression level was examined in the wild-type, *lpa1*, and Rev. plants before and after inoculation with *R. solani* AG1-IA. The qRT-PCR results showed that *PIN1a* was induced by *R. solani* AG1-IA inoculation, and the level was lower in *lpa1* than in the wild-type and Rev. plant leaves 72 h post-*R. solani* inoculation, but there were no significant differences without the inoculation (Fig. 1d).

IDD13 and IDD3 Interact with *LPA1*

Our transcriptome study discerned that several IDD genes, including *IDD3*, *IDD5*, *IDD10*, and *IDD13*, were differentially expressed upon *R. solani* infection (unpublished data). To verify the transcriptome data, qRT-PCR was performed to examine the expression of the *IDD* gene. The results showed that *IDD5* was suppressed, while *IDD3*, *IDD10*, and *IDD13* were induced by *R. solani* (Fig. 2a). To test whether *IDD3*, *IDD10*, or *IDD13* interact with *LPA1*, yeast two-hybrid, split-GFP, and co-immunoprecipitation (co-IP) assays were performed. A yeast-two hybrid analysis indicated that *LPA1* interacts with *IDD3* and *IDD13* but not with *IDD10* (Fig. 2b). An additional split-GFP assay showed that *LPA1* interacts with *IDD3* or *IDD13* at the nucleus in *N. benthamiana* leaves, but the negative control (*LPA1*-nYFP+cCFP) did not exhibit a visible signal (Fig. 2c). For the co-IP assay, *LPA1*-GFP was co-expressed with *IDD3*-Myc, *IDD13*-Myc or *IDD10*-Myc in *N. benthamiana* leaves, and the total proteins were immunoprecipitated using an anti-GFP antibody. The immunoprecipitated proteins were analyzed using an anti-Myc antibody. The results indicated that *LPA1* interacts with *IDD3* and *IDD13* but not *IDD10* in plants, and the interaction affinity in *LPA1*-*IDD13* was higher than that in *LPA1*-*IDD3* (Fig. 2d).

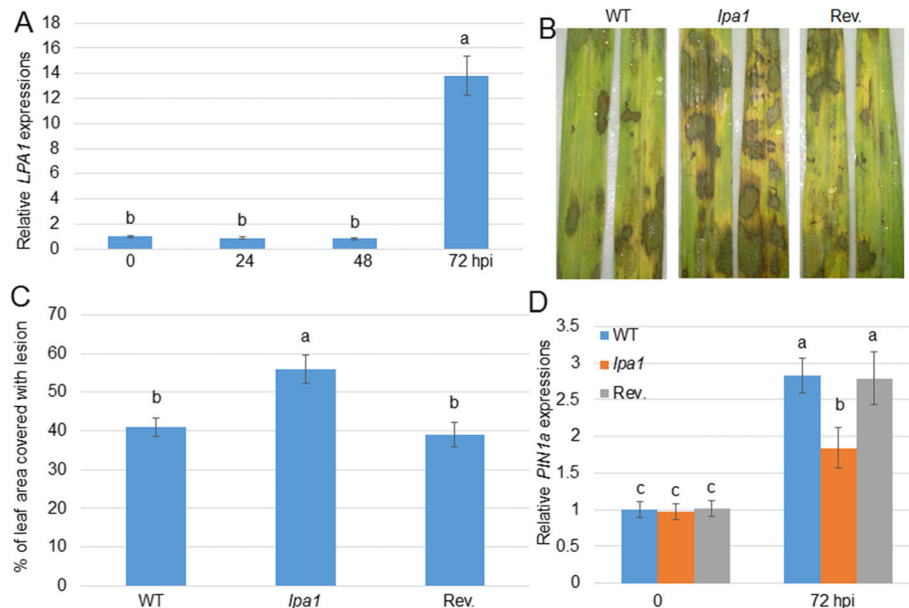


Fig. 1 *Rhizoctonia solani*-mediated *LPA1* expression patterns and *lpa1* mutant response to sheath blight disease. **a** *LPA1* expression level in the leaves at 0, 24, 48, and 72 h post-inoculation (hpi) of *R. solani* AG1-IA. The error bars are the mean \pm SE ($n = 3$). **b** Response of *lpa1* and revertant (Rev.) to *R. solani* AG1-IA compared with the wild-type (WT). **c** Percentage of the leaf area covered with lesions in *lpa1* and revertant (Rev.) compared with the WT. Data represent means \pm SE ($n > 10$). **d** *R. solani*-mediated expression of *PIN1a* in WT, *lpa1*, and Rev. leaves before and after 72 hpi of *R. solani*. Different letters indicate significant differences at $P < 0.05$

IDD3 Negatively and IDD13 Positively Regulated Resistance to Sheath Blight Disease

To analyze the function of IDD3 and IDD13 in response to ShB, *idd3* mutants (*idd3-1* and *idd3-2*), *IDD3* overexpressors (OX), *IDD13 RNAi*, and *IDD13 OX* plants were tested. Before examining their response to ShB, the levels of expression of *IDD3* and *IDD13* were analyzed. The qRT-PCR results showed that the *IDD3* transcript was not detected in two *idd3* knock-out mutants (*idd3-1* and *idd3-2*), while *IDD3* was highly expressed in the *IDD3 OX* plants (#2, #3, #4, and #6) compared with the wild-type control (Fig. 3a). In addition, *IDD13* was significantly suppressed in the *IDD13 RNAi* lines (#1, #2, #4, and #5), while it was obviously highly expressed in the *IDD13 OX* plants (#2, #3, #5, and #7) compared with the wild-type control (Fig. 3b). An additional *R. solani* infection test showed that the *idd3* mutants were similar to the wild-type control and displayed a susceptible response to *R. solani* AG1-IA, but *IDD3 OX* exhibited more susceptible symptoms than those in the wild-type plants. The percentage of the leaf area covered with lesions was 41% in WT, 42% in *idd3-1*, 40.5% in *idd3-2*, 54.5% in *IDD3 OX* #2, and 56% in *IDD3 OX* #4 plants (Fig. 3c and d). In addition, the *R. solani* infection results indicated that the *IDD13 RNAi* plants were more susceptible, while the *IDD13 OX* plants were less susceptible to ShB than the wild-type control. The percentage of leaf area covered with lesions

was 39% in the WT, 48% in *IDD13 RNAi* #1, 49% in *IDD13 RNAi* #4, 31% in *IDD13 OX* #2, and 30% in *IDD13 OX* #5 plants (Fig. 3e and f).

IDD3 and IDD13 Directly Regulate *PIN1a* Transcription

LPA1 promotes the resistance of rice to ShB via the activation of *PIN1a* (Sun et al., 2019), and *IDD3* and *IDD13* interact with *LPA1* to regulate the resistance to ShB. Therefore, we tested the potential of *IDD3* and *IDD13* to bind to the *PIN1a* promoter in more detail using a chromatin immunoprecipitation (ChIP) assay. Before performing the ChIP assay, the *IDD3-GFP* and *IDD13-GFP* localization in the transgenic plants was evaluated. The GFP signal was detected in the nucleus of *IDD3-GFP* and *IDD13-GFP* transgenic lateral roots (Fig. 4a). In the *PIN1a* promoter region, a single *IDD*-binding motif was identified (Fig. 4b). To examine whether *IDD3* and *IDD13* bind to the *IDD*-binding motif, a ChIP assay was performed using *35S:IDD3:GFP* or *35S:IDD13:GFP* transgenic plant calli and an anti-GFP antibody. The samples without the application of the GFP antibody (-Ab) were used as the control for the GFP antibody (+Ab) to immunoprecipitate the DNA. The ChIP-PCR results showed that *IDD3* and *IDD13* bound to the P2 but not to the P1 (Fig. 4c). An electrophoretic mobility shift assay (EMSA) was performed to verify that *IDD3* and *IDD13* bound the P2 fragment. The results indicated that *IDD3* and *IDD13* bound to P2, but the complex failed to bind to the mutated putative *IDD*-binding motif (TTTGTCG mutated to AAAAAAA) mP2 (Fig. 4d). To verify

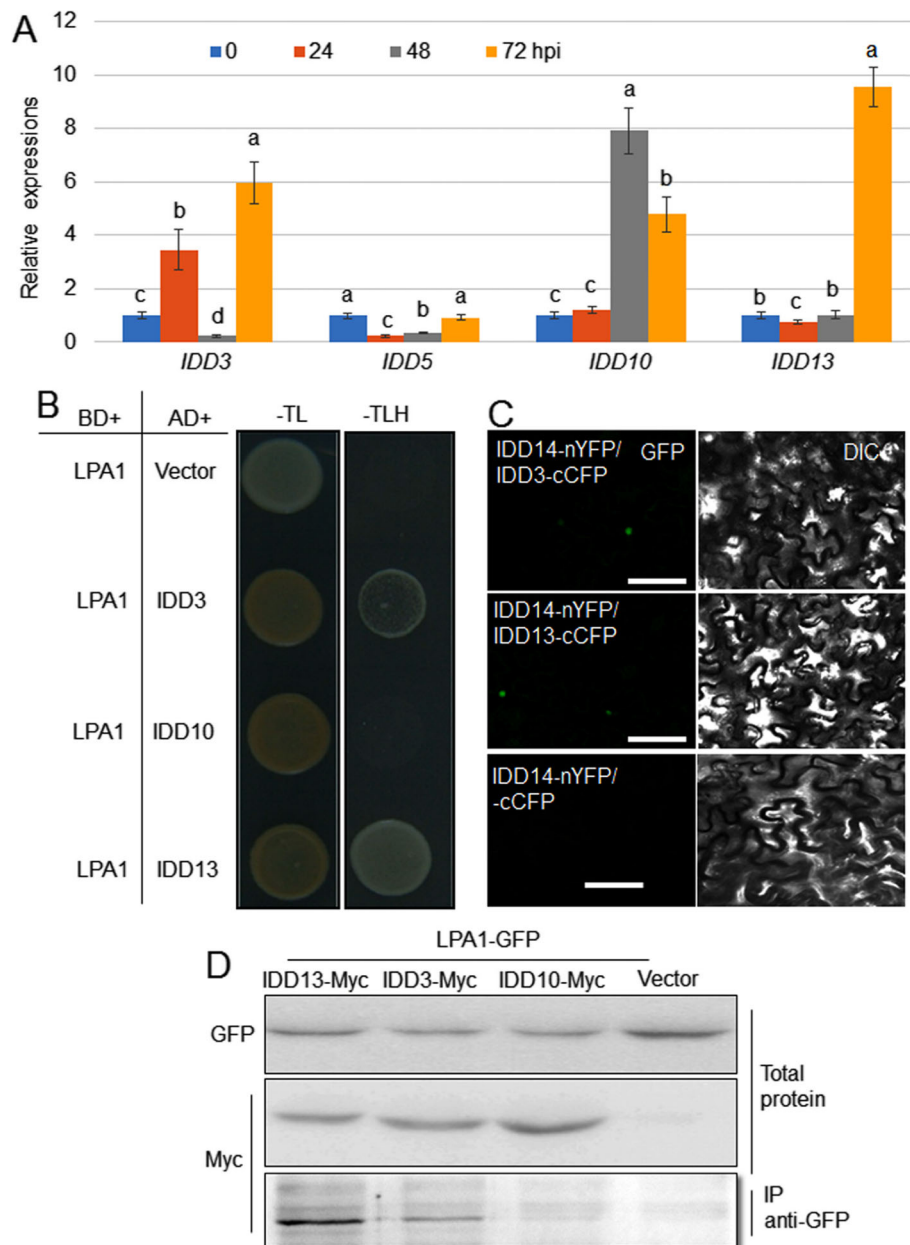
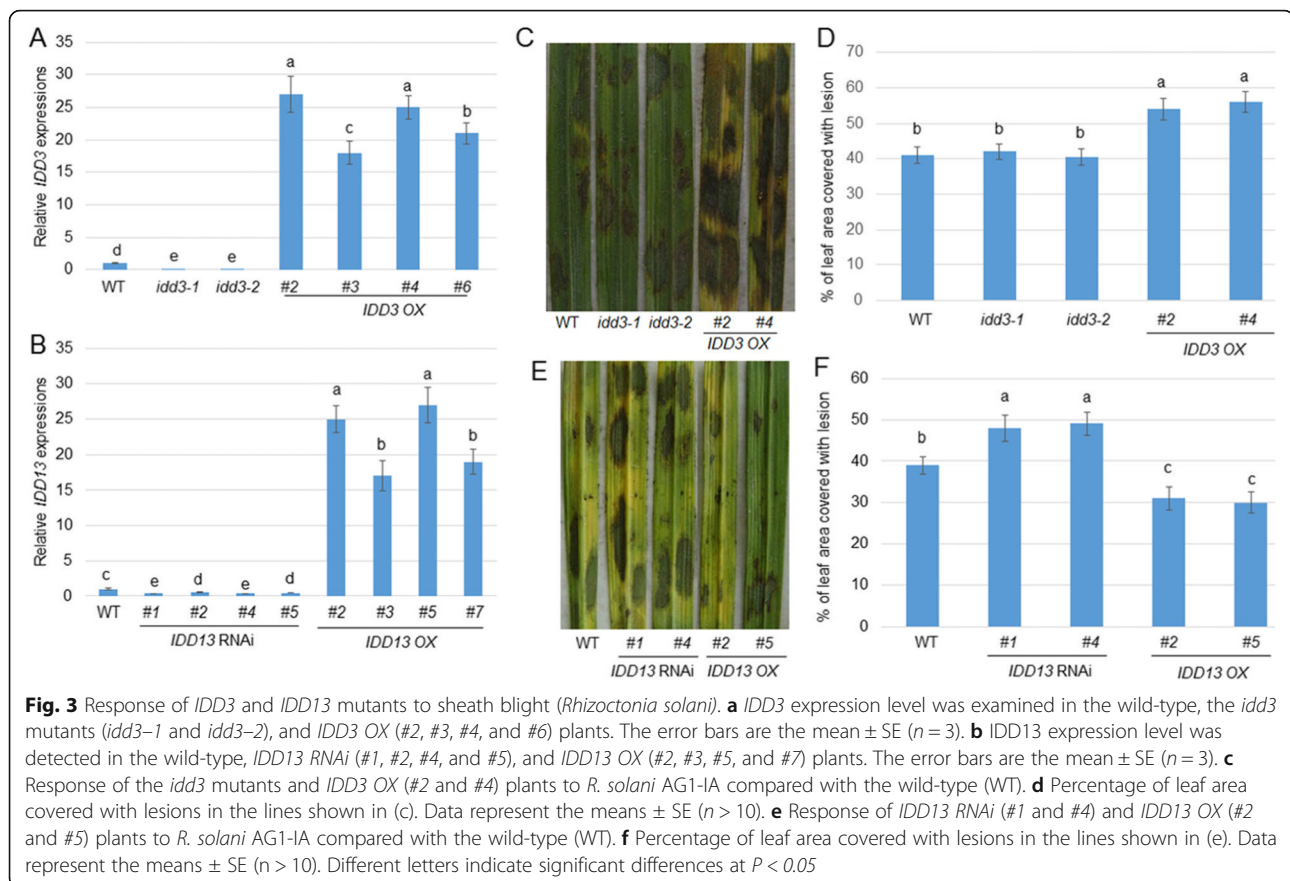


Fig. 2 Interaction between LPA1 and IDD3 or IDD13. **a** *IDD3*, *IDD5*, *IDD10*, and *IDD13* expression levels in the leaves at 0, 24, 48, and 72 h post-inoculation (hpi) of *Rhizoctonia solani* AG1-IA. The error bars are the mean \pm SE ($n = 3$). The statistical analysis was performed for each gene, and different letters indicate significant differences at $P < 0.05$. **b** A yeast two-hybrid assay was performed to analyze the interaction between LPA1 and *IDD3*, *IDD10*, or *IDD13*. BD: GAL4-DNA binding domain; AD: activation domain; -T: without tryptophan; -L: without leucine; -H: without histidine. **c** Reconstitution of GFP fluorescence from LPA1-nYFP + *IDD3*-cCFP, LPA1-nYFP + *IDD13*-cCFP, and LPA1-nYFP + cCFP. Bars = 10 μ m. DIC: differential interference contrast. **d** A co-IP assay was performed to analyze the interaction between LPA1 and *IDD3*, *IDD13*, or *IDD10* in tobacco leaves. *IDD3*-Myc, *IDD13*-Myc, *IDD10*-Myc + LPA1-GFP, or empty vector + LPA1-GFP were transformed into tobacco leaves using *Agrobacterium*-mediated transformation. Green fluorescent protein (GFP) antibody-immunoprecipitated proteins were analyzed using western blot analysis with the Myc antibody. *IDD3*-Myc, *IDD13*-Myc, *IDD10*-Myc, and LPA1-GFP levels were analyzed by western blot using Myc and GFP antibodies, respectively

the *IDD3* and *IDD13* activation of *PIN1a* via binding to the P2 region in the promoter, transient expression assays were conducted using the protoplast system. Protoplast cells were co-transformed with the *35S:IDD3* or *35S:IDD13* plasmid and

the construct expressing the β -glucuronidase gene (*GUS*) under the control of *pPIN1a* or *mpPIN1a*. In the mutated promoter (*mpPIN1a*), the *IDD*-binding motif sequences TTTGTTCG were replaced with AAAAAA. Protoplast cells



expressing *IDD3* had approximately twice the levels of activated *pPIN1a*. However, *IDD3* was unable to activate *mpPIN1a*. In parallel, *IDD3* suppressed *pPIN1a* by approximately one third but did not affect *mpPIN1a* (Fig. 4e).

In addition, the *PIN1a* expression level was examined in the *idd3* mutants and *IDD3 OX*, as well as in the *IDD13 RNAi* and *IDD13 OX* plants. The qRT-PCR results showed that the *PIN1a* level was obviously lower in *IDD3 OX* than in the wild-type and *idd3* mutants, but there were no significant differences between the wild-type and *idd3* mutants (Additional file 1: Figure S1a). Moreover, the *PIN1a* level was slightly lower in the *IDD13 RNAi* plants, while it was significantly higher in the *IDD13 OX* plants than in the wild-type control (Additional file 1: Figure S1b).

IDD3 Inhibits the LPA1-Mediated Activation of *PIN1a* Expression

IDD3 and *IDD13* interact with *LPA1*, and *IDD13* and *LPA1* directly activate *PIN1a* transcription, while *IDD3* suppresses it. Therefore, the effects of *IDD3* on *IDD13* and *LPA1* regulation on *PIN1a* expression were examined. To verify the effect, *35S:LPA1* was co-transformed with *35S:IDD13* or *35S:IDD3* and a vector expressing *GUS* under the control of *pPIN1a*. The results indicated that *IDD13* and *LPA1*

activated *pPIN1a*, while *IDD3* suppressed *pPIN1a*. In addition, co-expressing *IDD3* and *LPA1* increased the activation of *pPIN1a* compared to expressing the single *IDD* protein. However, the expression of *IDD3* inhibited the *LPA1* activation of *pPIN1a* (Fig. 5a). In addition, the possibility that *IDD3*, *IDD13*, and *LPA1* form a transcriptional complex was tested. *IDD3-HA* and *IDD13-Myc* were expressed in *N. benthamiana* leaves and immunoprecipitated using an anti-HA antibody, but the western blot results indicated that *IDD3* did not interact with *IDD13* (Fig. 5b). Additional *IDD3-HA*, *IDD13-Myc*, and *LPA1-GFP* proteins were expressed in *N. benthamiana* leaves, and the total protein was immunoprecipitated with an anti-HA antibody. The Co-IP results showed that *IDD3*, *IDD13*, and *LPA1* form a transcriptional complex in plants (Fig. 5b).

IDD13 Additively Functions with *LPA1* in the Regulation of Resistance to Sheath Blight Disease

The *IDD13 RNAi* and *lpa1* mutants were more susceptible to ShB, while the *idd3* mutants exhibited no significant differences compared to the wild-type control, suggesting that *IDD13* and *LPA1* but not *IDD3* might play a major role in the resistance of rice to ShB. To analyze whether *IDD13* and *LPA1* are functionally additive in the regulation of the resistance of rice to ShB, two genetic combinations were generated,

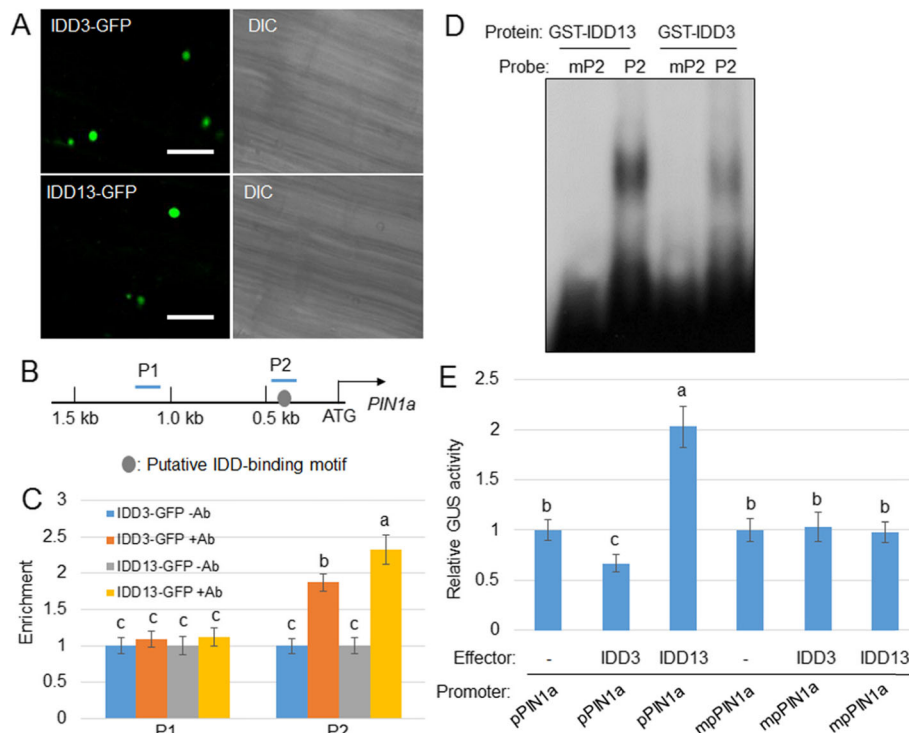


Fig. 4 IDD3 and IDD13 bind and activate the *PIN1a* promoter. **a** IDD3-GFP and IDD13-GFP were detected in the lateral roots. GFP signal and bright field are shown in the left and right, respectively. Bars = 20 μ m. **b** Schematic diagram indicating the location of the putative IDD-binding motif (gray circle) within 1.5 kb of the *PIN1a* promoter and the probes (P) used for chromatin immunoprecipitation (ChIP) assays. **c** Relative ratios of immunoprecipitated DNA to input DNA were determined by qPCR. Input DNA was used to normalize the data. -Ab or +Ab: green fluorescent protein (GFP) antibody. Error bars represent the mean \pm SE ($n = 3$). **d** An electrophoretic mobility-shift assay (EMSA) was conducted to evaluate GST-IDD3 and GST-IDD13 affinities to P2 and mutated probe mP2. **e** A transient expression assay was conducted by co-transfection with *p35S:IDD3* or *p35S:IDD13* and each of the vectors expressing *GUS* under the control of native (*pPIN1a*) and IDD-binding motif-mutated (*mpPIN1a*) *PIN1a* promoters in protoplast cells. The luciferase gene driven by the 35S promoter was used as an internal control to normalize *GUS* expression. Error bars represent the mean \pm SE ($n = 6$). Different letters indicate significant differences at $P < 0.05$

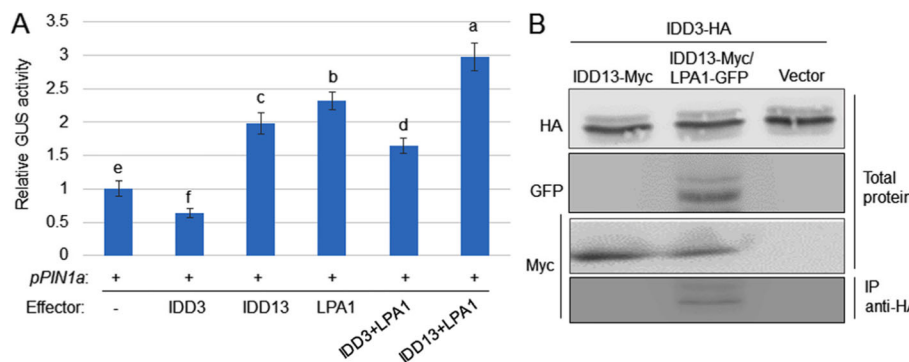


Fig. 5 IDD3, IDD13, and LPA1 form a complex to regulate *PIN1a* transcription. **a** A transient expression assay was conducted by co-transfection with *p35S:IDD3*, *p35S:IDD13*, *p35S:LPA1*, *p35S:IDD3 + p35S:LPA1*, *p35S:IDD13 + p35S:LPA1* and the vector expressing the *GUS* under the control of native (*pPIN1a*) *PIN1a* promoters in protoplast cells. The luciferase gene driven by the 35S promoter was used as an internal control to normalize the *GUS* expression. Error bars represent the mean \pm SE ($n = 6$). Different letters indicate significant differences at $P < 0.05$. **b** IDD3-HA + IDD13-Myc, IDD3-HA + IDD13-Myc + LPA1-GFP, or IDD3-HA + empty vector were transformed into tobacco leaves using *Agrobacterium*-mediated transformation. HA antibody-immunoprecipitated proteins were analyzed using western blot analysis with the Myc antibody. IDD3-HA, IDD13-Myc, and LPA1-GFP levels were analyzed by a western blot using HA, Myc, and GFP antibodies, respectively

including *IDD13 RNAi/lpa1* and *lpa1/IDD13 OX*. In addition, *LPA1* repressor lines were examined (Wu et al. 2013, Liu et al. 2016). An *R. solani* infection test showed that *IDD13 RNAi/lpa1* was more susceptible than the *IDD13 RNAi*, *lpa1*, and wild-type plants segregated from the same sibling, and *IDD13 RNAi/lpa1* exhibited similar susceptible symptoms to the *LPA1* repressor (Fig. 6a). The percentage of the leaf area covered with lesions was 41% in the WT, 51% in *IDD13 RNAi*, 54% in *lpa1*, 63% in *IDD13 RNAi/lpa1*, and 61.5% in the *LPA1* repressor plants (Fig. 6b). In addition, *R. solani* infection results indicated that the *lpa1/IDD13 OX* plants were less susceptible to ShB than the *lpa1* mutant and wild-type segregated from the same sibling, but they were more susceptible to ShB compared to the *IDD13 OX* plants segregated from the same sibling (Fig. 6c). The percentage of leaf area covered with lesions was 40.5% in WT, 53% in *lpa1*, 32% in *IDD13 OX*, and 37.5% in *lpa1/IDD13 OX* plants (Fig. 6d).

In addition, the level of expression of *PIN1a* was examined in the *IDD13 RNAi/lpa1*, *lpa1/IDD13 OX*, and *LPA1* repressor lines. The qRT-PCR results showed that the *PIN1a* level was much lower in *IDD13 RNAi/lpa1* than in the wild-type,

IDD13 RNAi, and *lpa1* and was similar between *IDD13 RNAi/lpa1* and the *LPA1* repressor after *R. solani* inoculation (Additional file 2: Figure S2a). In parallel, the *PIN1a* level was higher in *lpa1/IDD13 OX* than in *lpa1* and higher than in the wild-type plants. The *PIN1a* level was noticeably higher in *IDD13 OX* than in the wild-type and *lpa1/IDD13 OX* after *R. solani* inoculation (Additional file 2: Figure S2b).

IDD13 Overexpression Maintained Yield Production in Rice

Since the *IDD13 OX* plants demonstrated increased resistance to ShB, yield factors were investigated further. The results demonstrated that *IDD13 OX* plants developed a similar tiller number, thousand-grain weight, and number of spikelets per panicle relative to the WT, but the overexpression of *IDD13* slightly decreased the tiller angle compared with the wild-type (WT) plants (Fig. 7). *LPA1* overexpression increased the content of 3-indole acetic acid (IAA), a natural form of auxin, and exogenous IAA treatment promoted the resistance of rice to ShB (Sun et al. 2019). Therefore, the endogenous IAA

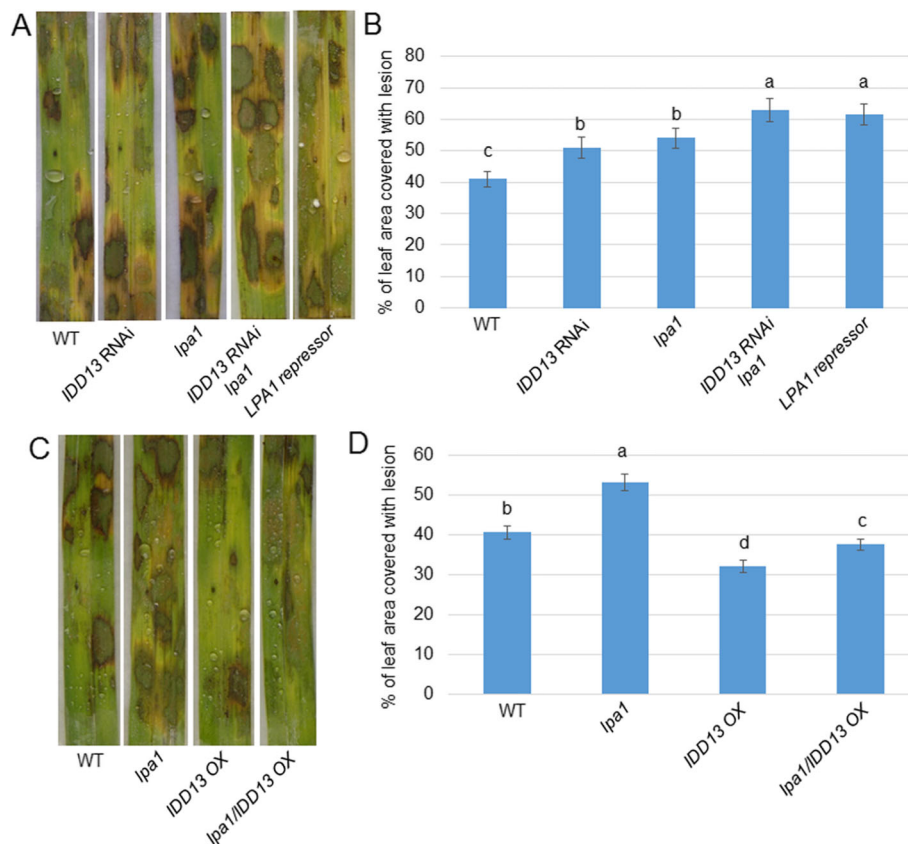


Fig. 6 *IDD13* and *LPA1* genetic combinations in response to sheath blight (*Rhizoctonia solani*). **a** Response of *IDD13 RNAi*, *lpa1*, *IDD13 RNAi/lpa1*, *LPA1* repressor plants to *R. solani* AG1-IA compared with the wild-type (WT). **b** Percentage of the leaf area covered with lesions in the lines shown in (a). Data represent the means \pm SE ($n > 10$). **c** Response of the *lpa1*, *IDD13 OX*, and *lpa1/IDD13 OX* plants to *R. solani* AG1-IA compared with the wild-type (WT). **d** Percentage of the leaf area covered with lesions in the lines shown in (c). Data represent the means \pm SE ($n > 10$). Different letters indicate significant differences at $P < 0.05$

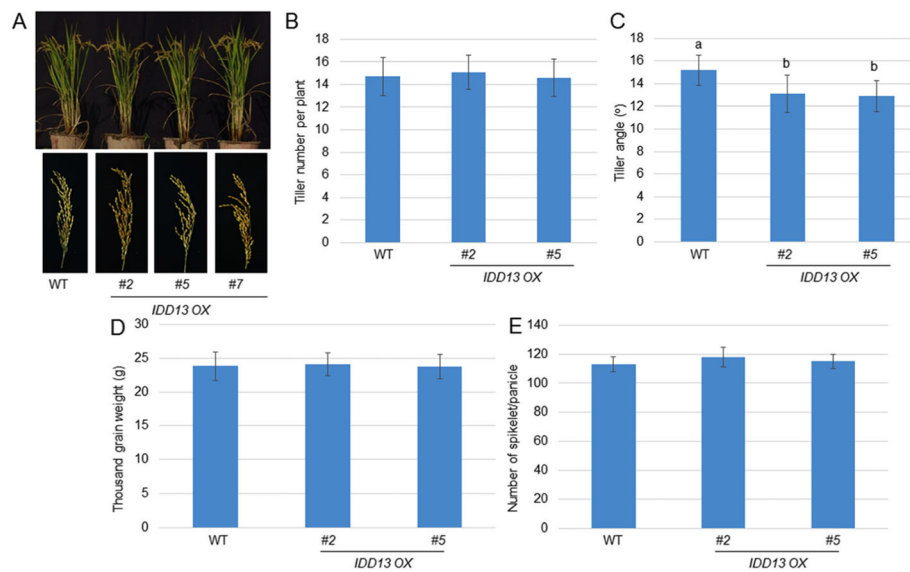


Fig. 7 The tiller number, thousand-grain weight and number of spikelet per panicle in the wild-type and *IDD13* OX plants. **a** The three-and-a-half-month-old wild-type and *IDD13* OX plants (#2, #5, and #7), as well as their panicles, are shown. Tiller number **b**, tiller angles **c**, thousand-grain weight **d**, and the number of grain weight per panicle **e** from the wild-type and *IDD13* OX plants (#2 and #5) were calculated. Data indicate the average \pm SD ($n > 15$). Different letters indicate significant differences at $P < 0.05$

levels in the WT, *IDD13* OX2, and *IDD13* OX5 plants were measured. The data demonstrated that *IDD13* overexpressors contain higher levels of IAA than that of the WT plant leaves (Additional file 3: Figure S3).

Discussion

Sheath blight disease caused by *R. solani* is a major rice disease, which severely reduces grain yield. However, the host resistance mechanisms remain unknown. Previously, we identified that exogenous auxin treatment promoted resistance to ShB, and the overexpression of *LPA1/IDD14* promoted rice defense to ShB via the activation of the auxin poplar transporter *PIN1a* in rice (Sun et al. 2019). *PIN1a* RNAi and the *PIN1a* overexpressors were more and less susceptible to ShB, respectively (Sun et al. 2019), suggesting that *LPA1* increases the local auxin content or the activation of auxin signaling by controlling *PIN1a* and enhancing the resistance of the rice to ShB. However, whether IDD proteins other than *LPA1* regulate the resistance of rice remains unclear.

IDDs Were Induced by *R. solani*, and *LPA1* Interacts with *IDD3* and *IDD13*

The transcriptome analysis and additional qPCR verification showed that *IDD3*, *IDD10*, *IDD13*, and *LPA1* were up-regulated, while *IDD5* was down-regulated by *R. solani* in rice. In normal conditions, *LPA1* is barely expressed in the leaves and sheath of rice (Wu et al. 2013), but *R. solani* infection significantly induced the level of expression of *LPA1* in the leaves. Additional genetic study showed that the *lpa1* and *IDD13* RNAi mutant were more susceptible, but the *idd3*

mutants exhibited a similar response to ShB compared with the wild-type. In addition, the overexpression of *IDD13* produced results similar to those of *LPA1*, whereas the overexpression of *IDD3* inhibited the resistance of rice to ShB, indicating that rice defense against ShB requires *LPA1* and *IDD13*, and *IDD3* negatively regulates the defense of rice to ShB. Since AtIDD15 functions in concert with AtIDD14 and AtIDD16 to directly activate auxin biosynthesis and transport-related genes in Arabidopsis (Cui et al. 2013), this suggests that IDD proteins are functionally additive in the regulation of auxin biosynthesis. Further biochemical and molecular assays identified that *LPA1* interacts with *IDD3* and *IDD13*, and the interaction affinity of *LPA1* was higher with *IDD13* than with *IDD3*. However, *IDD3* did not directly interact with *IDD13*, while *LPA1*, *IDD3*, and *IDD13* form a transcriptional complex, suggesting that these three *IDDs* may form a transcriptional complex to regulate the resistance of rice to ShB.

IDD13 Positively and *IDD3* Negatively Regulate *PIN1a*

LPA1 and *IDD10* were reported to localize to the nucleus and function as transcription factors (Wu et al. 2013; Xuan et al. 2013), and *IDD3*-GFP and *IDD13*-GFP were localized to the nucleus in the transgenic rice roots. Previously, we identified that *PIN1a* is a direct target of *LPA1*, which positively regulates the resistance of rice to ShB (Sun et al. 2019). Since *LPA1* interacts with *IDD3* and *IDD13*, the roles of *IDD3* and *IDD13* in the regulation of *PIN1a* transcription were analyzed. Additional ChIP and EMAS assays showed that *IDD13* and *IDD3* directly bound to the putative *IDD*-binding motif in the *PIN1a* promoter region. In addition, a transient assay

revealed that *IDD13* acted similarly to *LPA1* to directly activate *PIN1a*, but *IDD3* directly bound to the *PIN1a* promoter and functioned as a transcriptional repressor. The transient assay results showed that the expression of *IDD13* and *LPA1* activated the level of transcription of *PIN1a*, while the expression of *IDD3* suppressed the level of expression of *PIN1a*, suggesting that *IDD13* and *LPA1* function as transcriptional activators, while *IDD3* functions as a transcriptional repressor to *PIN1a*.

The overexpression of *LPA1* reduced the tiller angle and increased the contents of IAA in the leaves via the activation of *PIN1a* (Sun et al. 2019). *IDD13* activates *PIN1a*, and the additional investigation of yield factors identified that the overexpression of *IDD13* maintained yield production, while reducing the tiller angle compared with the wild-type plants. In addition, the *IDD13 OX* plants accumulated higher contents of IAA than were found in the wild-type plant leaves, suggesting that *IDD13 OX* acts similarly to the *LPA1 OX* plants to increase the resistance of rice to ShB by activating *PIN1a* without affecting rice production. However, the tiller angle of the *LPA1 OX* plants is smaller than that in the *IDD13 OX* plants, implying a dominant regulation of *LPA1* compared with *IDD13* in the transcriptional activation of *PIN1a*.

IDD13 and LPA1 Are Functionally Additive in the Regulation of the Resistance of Rice to Sheath Blight Disease

IDD3, *IDD13*, and *LPA1* physically interact with and differentially regulate *PIN1a*. In addition, *LPA1* positively regulates the resistance of rice to ShB. Next, a genetic study was performed to analyze the functions of *IDD3* and *IDD13* in the control of the resistance of rice to ShB. An *R. solani* infection assay indicated that the two *idd3* mutants exhibited a similar susceptible response to ShB compared with the wild-type control. In addition, the level of expression of *PIN1a* was not changed in the *idd3* mutants, which was similar to its expression in the wild-type plants. The overexpression of *IDD3* significantly suppressed the *PIN1a* level compared with the wild-type plants, and *IDD3 OX* exhibited more susceptible symptoms to *R. solani* infection than the wild-type plants. The *IDD13 RNAi* plants were more susceptible to ShB, while the *IDD13 OX* plants were less susceptible compared with the wild-type plants. In addition, the *PIN1a* expression level was lower in the *IDD13 RNAi* and higher in the *IDD13 OX* plants than in the wild-type plants, suggesting that *IDD13* might regulate the resistance to ShB via the activation of *PIN1a*. The *IDD3* mutation did not change the resistance of the rice to ShB, as well as the *PIN1a* expression, implying that *IDD3* might not be a major regulator of *PIN1a* transcription.

IDD13 and *LPA1* interact and activate *PIN1a* transcription. In addition, the *IDD3 RNAi* and *lpa1* mutants

were more susceptible to ShB, while the *IDD13 OX* and *LPA1 OX* plants were less susceptible compared with the wild-type control. Further genetic and pathology experiments indicated that an *IDD13 RNAi/lpa1* double mutant was more susceptible to ShB compared with *IDD13 RNAi* and *lpa1*. In addition, the response of the *LPA1* repressor plants to ShB was compared with that of *IDD13 RNAi/lpa1*. The results showed that expressing the *LPA1* repressor to inhibit the transcription complex, including *LPA1*, produced a similar defect in response to ShB when compared with *IDD13 RNAi/lpa1*, and showed more susceptible symptom than in *lpa1* and *IDD13 RNAi*, suggesting that *IDD13* and *LPA1* might be functionally additive. In parallel, the *lpa1/IDD13 OX* double mutants were more susceptible to ShB compared with the *IDD13 OX* plants, but they were less susceptible to ShB compared to *lpa1* and the wild-type control, suggesting that *IDD13 OX* can partially rescue the defect from the *LPA1* mutation in response to ShB. Additional expression level analyses indicated that the level of *PIN1a* was much lower in *IDD13 RNAi/lpa1* or the *LPA1* repressor than in *IDD13 RNAi* and *lpa1*, while it was higher in *lpa1/IDD13 OX* than in *lpa1*. These results suggest that *IDD13* and *LPA1* might be functionally additive in the regulation of the resistance of rice to ShB via the activation of *PIN1a* expression in rice.

Overall, this study identified a new *IDD* transcriptional complex and identified its function in the regulation of ShB via the regulation of *PIN1a* transcription. These results will broaden our understanding of the regulatory mechanism by which the *IDDs* regulate auxin transport and the resistance of rice to ShB.

Methods

Plant Growth and *R. solani* AG1-IA Inoculation

Wild-type (WT) control line (*Oryza sativa* Japonica, cultivar Dongjin), *lpa1*, *LPA1 revertant (Rev.)*, *IDD13 RNAi*, *IDD13-GFP* overexpressor (*IDD13 OX*), *idd3-1* (PFG_3A-09378), *idd3-2* (PFG_3A-14,411), *IDD3-GFP overexpressor (IDD3 OX)*, *lpa1/IDD13 RNAi*, *lpa1/IDD13 OX*, and *LPA1* repressor plants were used. The plants were grown in a greenhouse at Shenyang Agricultural University, China, with a temperature of 23 °C–30 °C. One-month-old rice plants were inoculated with *R. solani* AG1-IA (Prasad and Eizenga, 2008). In brief, a 10-cm-long piece was cut from the second youngest leaf of the main tiller and placed on moistened filter paper in a Petri dish (diameter, 36 cm; height, 2.5 cm). Each replicate comprised six leaves, and four replicates per leaf were used in a completely randomized design. Colonized potato dextrose agar (PDA) blocks (diameter, 7 mm) were excised using a circular cutter and placed on the abaxial surface of each leaf piece. The leaves were incubated at 25 °C for 72 h in a chamber with continuous

light. The filter paper was kept moist with sterile water. After 72 h, the length and width of the lesions within each leaf piece were measured using Image J Fiji software (NIH, Bethesda, MD, USA) and the approximate percentage of the leaf covered with lesions was calculated as previously described (Prasad and Eizenga, 2008; Eizenga et al. 2002). To analyze the *R. solani* AG1-IA infection-mediated expression of the *IDD* genes, one-month-old wild-type plants were inoculated with *R. solani* AG1-IA, and their leaves were sampled after 0, 24, 48, and 72 h of inoculation. The accession numbers in Genbank are as follows: *IDD3* (EEC85036), *IDD5* (XP_015647948), *IDD10* (KAB8096499), *IDD13* (XP_015610838), and *LPA1* (*IDD14*) (XP_015629419).

RNA Extraction and Quantitative Real-Time (qRT)-PCR Analysis

Total RNA was isolated from the one-month-old rice leaves using the TRIzol reagent (Takara, Dalian, China), and the genomic DNA was removed by treatment with RQ-RNase free DNase (Promega, Madison, WI, USA). Complementary DNA was synthesized using the GoScript Reverse Transcription Kit (Promega) following the manufacturer's instructions. A BIO-RAD CFX96 Real-time PCR system (Bio-Rad, Hercules, CA, USA) and SYBR-Green (Takara) were used for the qRT-PCR analyses. The gene expression levels were normalized to that of the level of *Ubiquitin*. The primers used for qRT-PCR are listed in Additional file 4: Table S1.

Plasmid Construction

To generate *IDD3-GFP* and *IDD13-GFP* overexpression transgenic plants, *IDD3* and *IDD13* ORF sequences were amplified and cloned into *Bgl*II and *Spe*I restriction enzyme sites of the pCAMBIA1302 binary vector, in which *IDD3* or *IDD13* coding sequences were N-terminally fused to the *GFP* coding sequences. To generate *IDD13 RNAi* plants, 300 bp of the *IDD13* coding region was cloned into *Swa*I and *Asc*I sites in the sense and *Xba*I and *Bam*HI sites in the antisense orientation, respectively, in the pFGC5941 binary vector (ChromDB).

Yeast Two-Hybrid Assay

To test the interaction between *LPA1* and *IDD13*, *IDD3* or *IDD10*, the Gal4 DNA-binding domain (BD) was N-terminally fused to *LPA1*, while *IDD13*, *IDD3*, or *IDD10* ORFs were cloned into the pGAD424 vector. The pair of *IDDs* was further transformed in the yeast strain PJ69-4A (Clontech, <http://www.clontech.com/>). Yeast cells carrying a pair of *IDDs* were grown on SD/Trp⁻/Leu⁻ and SD/Trp⁻/Leu⁻/His⁻ plates. The sequences of the primers for cloning the *IDD13* ORF are listed in Additional file 3: Table S1.

Split GFP Assay

The N-proximal half of YFP (nYFP) and the C-proximal half of CFP (cCFP) sequences were fused to the C-terminal sequences of *LPA1* (*IDD14*) and C-terminal sequences of *IDD3* or *IDD13* in the pXNGW and pXCGW vectors, respectively. Agrobacterium cells (GV3101) harboring half of the YFP parts were mixed and then infiltrated into *Nicotiana benthamiana* leaves. Before observing the YFP signal using a confocal microscope (Olympus X1000, Japan), the tobacco plants were grown in a growth chamber for 36 to 48 h (Kim et al. 2009a).

Co-Immunoprecipitation (co-IP) and Western Blot Analyses

IDD3-Myc + LPA1-GFP, *IDD13-Myc + LPA1-GFP*, *IDD10-Myc + LPA1-GFP*, *IDD3-HA + IDD13-Myc*, or *IDD3-HA + IDD13-Myc + LPA1-GFP* were coexpressed in *N. benthamiana* leaves, respectively. After 36 h of expression, the protein was extracted, and Co-IP assays were performed as described previously (Kim et al. 2009b). Twenty micrograms of protein from each sample were separated on a 10% SDS-PAGE gel and electrotransferred onto Immobilon-P Transfer Membranes (MILLIPORE JAPAN, Tokyo, Japan). For the subsequent western blot analysis, the following primary antibodies were used: an anti-HA antibody (1:2000; Abcam, Cambridge, MA, USA), anti-GFP antibody (1:2000; Abcam), and anti-Myc antibody (1:2000; Abcam). The membranes were incubated for an additional hour with an anti-mouse or anti-rabbit horseradish peroxidase (HRP)-conjugated secondary antibody (1:2000; Cell Signaling Technology, Danvers, MA, USA) before the signal was detected using an ECL Western Blotting Detection System (GE Healthcare, Piscataway, NJ, USA).

Chromatin-Immunoprecipitation (ChIP) Assay

Eight grams of rice calli were collected from transgenic plants expressing *35S:IDD13-GFP* and *35S:IDD3-GFP* for the ChIP assay. The ChIP assay and subsequent ChIP-PCR assays were followed by a protocol described previously (Je et al. 2010). The primers used for the ChIP-PCR are listed in Additional file 3: Table S1.

Electrophoretic Mobility Shift Assay (EMSA)

To produce *IDD13* and *IDD3* recombinant proteins, the open reading frame sequences of *IDD13* and *IDD3* were sub-cloned into the *pGEX 5X-1* expression vector, and the resulting *pGEX 5X-1-IDD13* and *pGEX 5X-1-IDD3* plasmids were used to transform *Escherichia coli* strain BL21 DE3. Recombinant proteins were harvested after a 4 h treatment with 0.5 mM isopropyl β-D-1-thiogalactopyranoside (IPTG) at 28 °C. The EMSA was performed as previously described (Je et al. 2010). The primers used to obtain the EMSA probes are listed in Additional file 3: Table S1.

Transient Expression Assay

For the transient assay, the effector plasmids (*35S:LPA1*, *35S:IDD13*, and *35S:IDD3*) and reporter (*pPIN1a* or mutated promoter, *mpPIN1a*), as well as an internal control plasmid (*35S:LUC*), were co-transformed into protoplast cells (Yamaguchi et al. 2010). The GUS activity analyses were performed as previously described (Xuan et al. 2013). The luciferase assay was performed using a Luciferase Assay Kit (Promega), and PEG-mediated transformation and luciferase activity assays were performed as previously described (Yoo et al. 2007). The primers used for the transient assay are listed in Additional file 3: Table S1.

IAA Measurement

The leaves from 1-month-old *IDD13 OX2*, *IDD13 OX5*, and wild-type plants were used for IAA extraction. IAA extraction and calculation methods were followed as described by Pan et al. (2010). IAA-[α , α -D2] was used as an internal standard of IAA in the experiments.

Statistical Analyses

Statistical analyses were performed using Prism 5.0 (GraphPad, San Diego, CA, USA). For multiple lines comparison, a one-way analysis of variance (ANOVA) was performed, followed by Bonferroni's multiple comparison tests. Differences among the samples were considered significant at $P < 0.05$.

Supplementary information

Supplementary information accompanies this paper at <https://doi.org/10.1186/s12284-020-0371-1>.

Additional file 1: Figure S1. *PIN1a* expression in *IDD3* and *IDD13* mutants and overexpressors. (A) Relative expression of *PIN1a* in wild-type (WT), *idd3-1*, *idd3-2*, *IDD3 OX #2*, and *IDD3 OX #4* plant leaves. (B) Relative expression of *PIN1a* in wild-type (WT), *IDD13 RNAi* (#1 and #4), *IDD3 OX #2*, and *IDD3 OX #5* plant leaves. The mRNA levels of the samples were normalized to that of *Ubiquitin* mRNA. Data represent the means \pm standard error ($n = 3$). The expression of *PIN1a* in the WT was defined as "1". Different letters indicate significant differences at $P < 0.05$.

Additional file 2: Figure S2. *PIN1a* expression in *LPA1* and *IDD13* genetic combinations. (A) Relative expression of *PIN1a* in the wild-type (WT), *IDD13 RNAi*, *lpa1*, *IDD13 RNAi/lpa1* and *LPA1 repressor* plant leaves after 72 h of *Rhizoctonia solani* inoculation. (B) Relative expression of *PIN1a* in the wild-type (WT), *lpa1*, *IDD3 OX*, and *lpa1/IDD3 OX* plant leaves after 72 h of *R. solani* inoculation. The mRNA levels of the samples were normalized to that of *Ubiquitin* mRNA. Data represent the means \pm standard error ($n = 3$). The expression of *PIN1a* in WT was defined as "1". Different letters indicate significant differences at $P < 0.05$.

Additional file 3: Figure S3. Measurement of the IAA content in WT and *IDD13* overexpressors. The contents of IAA from the leaves of 1-month-old WT and *IDD13 OX* lines (*OX2* and *OX5*) were measured. Vertical bars indicate average values \pm SE ($n = 3$). Different letters indicate significant differences at $P < 0.05$.

Additional file 4: Table S1. Primer sequences

Abbreviations

ChIP: Chromatin-Immunoprecipitation; DIC: Differential Interference Contrast; EMSA: Electrophoretic Mobility Shift Assay; IDD: Indeterminate Domain;

LPA1: Loose Plant Architecture1; OX: Overexpressor; PIN1a: Pin-Formed 1a; ShB: Sheath Blight Disease; WT: Wild Type

Acknowledgements

The authors would thank Dr. Chang-deok Han at Gyeongsang National University, Korea for providing rice seeds.

Authors' Contributions

Q Sun, and YH Xuan designed the experiment and wrote the manuscript. Q Sun, DD Li, J Chu, DP Yuan, and X Han conducted the experiments and performed data analysis. S Li, and LJ Zhong participated in material development, sample preparation and data analysis. Q Sun, X Han, and YH Xuan corrected the manuscript. All authors read and approved the final manuscript.

Funding

This work was supported by an initiative grant (880416008) from Shenyang Agricultural University, the Support Plan for Innovative Talents in Colleges and Universities of Liaoning Province (LR2017037), and National Key R&D Program of China (2016YFD0101004).

Availability of Data and Materials

The datasets supporting the conclusions of this article are provided within the article and its additional files.

Ethics Approval and Consent to Participate

Not applicable.

Consent for Publication

Not applicable.

Competing Interests

The authors declare that they have no competing interests.

Author details

¹College of Plant Protection, Shenyang Agricultural University, Shenyang 110866, China. ²Institute of Plant Protection, Liaoning Academy of Agricultural Sciences, Shenyang 110161, China. ³Shaanxi Key Laboratory of Chinese Jujube, Yan'an University, Yan'an 716000, Shaanxi, China. ⁴College of Life Science, Yan'an University, Yan'an 716000, Shaanxi, China. ⁵Microbial Research Institute, Liaoning Academy of Agricultural Sciences, Chaoyang 122000, China. ⁶College of Biological Science and Engineering, Fuzhou University, Fuzhou 350108, China.

Received: 24 October 2019 Accepted: 28 January 2020

Published online: 06 March 2020

References

- Adamowski M, Friml J (2015) PIN-dependent auxin transport: action, regulation, and evolution. *Plant Cell* 27(1):20–32
- Chen Z, Agnew JL, Cohen JD, He P, Shan L, Sheen J, Kunkel BN (2007) *Pseudomonas syringae* type III effector AvrRpt2 alters Arabidopsis thaliana auxin physiology. *Proc Natl Acad Sci U S A* 104(50):20131–20136
- Colasanti J, Yuan Z, Sundaresan V (1998) The indeterminate gene encodes a zinc finger protein and regulates a leaf-generated signal required for the transition to flowering in maize. *Cell* 93(4):593–603
- Cui D, Zhao J, Jing Y, Fan M, Liu J, Wang Z, Xin W, Hu Y (2013) The Arabidopsis IDD14, IDD15, and IDD16 cooperatively regulate lateral organ morphogenesis and gravitropism by promoting auxin biosynthesis and transport. *PLoS Genet* 9(9):e1003759
- Dou M, Cheng S, Zhao B, Xuan Y, Shao M (2016) The indeterminate domain protein ROC1 regulates chilling tolerance via activation of DREB1B/CBF1 in Rice. *Int J Mol Sci* 17(3):233
- Eizenga GC, Lee FN, Rutger JN (2002) Screening Oryza species plants for Rice sheath blight resistance. *Plant Dis* 86(7):808–812
- Feurtado JA, Huang D, Wicki-Stordeur L, Hemstock LE, Potentier MS, Tsang EW, Cutler AJ (2011) The Arabidopsis C2H2 zinc finger INDETERMINATE DOMAIN1/ENHYDROUS promotes the transition to germination by regulating light and hormonal signaling during seed maturation. *Plant Cell* 23(5):1772–1794
- Fu J, Liu H, Li Y, Yu H, Li X, Xiao J, Wang S (2011) Manipulating broad-spectrum disease resistance by suppressing pathogen-induced auxin accumulation in rice. *Plant Physiol* 155(1):589–602

- Gao Y, Zhang C, Han X, Wang ZY, Ma L, Yuan P, Wu JN, Zhu XF, Liu JM, Li DP, Hu YB, Xuan YH (2018) Inhibition of OsSWEET11 function in mesophyll cells improves resistance of rice to sheath blight disease. *Mol Plant Pathol* 19(9):2149–2161
- Helliwell EE, Wang Q, Yang Y (2013) Transgenic rice with inducible ethylene production exhibits broad-spectrum disease resistance to the fungal pathogens *Magnaporthe oryzae* and *Rhizoctonia solani*. *Plant Biotechnol J* 11(1):33–42
- Huang P, Yoshida H, Yano K, Kinoshita S, Kawai K, Koketsu E, Hattori M, Ordonio RL, Matsuoka M, Ueguchi-Tanaka M (2018) OsIDD2, a zinc finger and INDETERMINATE DOMAIN protein, regulates secondary cell wall formation. *J Integr Plant Biol* 60(2):130–143
- Je BI, Piao HL, Park SJ, Park SH, Kim CM, Xuan YH, Park SH, Huang J, Do Choi Y, An G, Wong HL, Fujioka S, Kim MC, Shimamoto K, Han CD (2010) RAV-Like1 maintains brassinosteroid homeostasis via the coordinated activation of BRI1 and biosynthetic genes in rice. *Plant Cell* 22(6):1777–1791
- Kim JG, Li X, Roden JA, Taylor KW, Aakre CD, Su B, Lalonde S, Kirik A, Chen Y, Baranage G, McLane H, Martin GB, Mudgett MB (2009a) Xanthomonas T3S effector XopN suppresses PAMP-triggered immunity and interacts with a tomato atypical receptor-like kinase and TFT1. *Plant Cell* 21(4):1305–1323
- Kim TW, Guan S, Sun Y, Deng Z, Tang W, Shang JX, Sun Y, Burlingame AL, Wang ZY (2009b) Brassinosteroid signal transduction from cell-surface receptor kinases to nuclear transcription factors. *Nat Cell Biol* 11(10):1254–1260
- Kouzai Y, Kimura M, Watanabe M, Kusunoki K, Osaka D, Suzuki T, Matsui H, Yamamoto M, Ichinose Y, Toyoda K, Matsuura T, Mori IC, Hirayama T, Minami E, Nishizawa Y, Inoue K, Onda Y, Mochida K, Noutoshi Y (2018) Salicylic acid-dependent immunity contributes to resistance against *Rhizoctonia solani*, a necrotrophic fungal agent of sheath blight, in rice and *Brachypodium distachyon*. *New Phytol* 217(2):771–783
- Kozaki A, Hake S, Colasanti J (2004) The maize ID1 flowering time regulator is a zinc finger protein with novel DNA binding properties. *Nucleic Acids Res* 32(5):1710–1720
- Liu JM, Park SJ, Huang J, Lee EJ, Xuan YH, Je BI, Kumar V, Priatama RA, Raj KV, Kim SH, Min MK, Cho JH, Kim TH, Chandran AK, Jung KH, Takatsuto S, Fujioka S, Han CD (2016) Loose plant Architecture1 (LPA1) determines lamina joint bending by suppressing auxin signalling that interacts with C⁻²²-hydroxylated and 6-deoxy brassinosteroids in rice. *J Exp Bot* 67(6):1883–1895
- Maeda S, Dubouzet JG, Kondou Y, Jikumaru Y, Seo S, Oda K, Matsui M, Hirochika H, Mori M (2019) The rice CYP78A gene BSR2 confers resistance to *Rhizoctonia solani* and affects seed size and growth in *Arabidopsis* and rice. *Sci Rep* 9(1):587
- Mao B, Liu X, Hu D, Li D (2014) Co-expression of RCH10 and AGLU1 confers rice resistance to fungal sheath blight *Rhizoctonia solani* and blast *Magnaporthe oryzae* and reveals impact on seed germination. *World J Microbiol Biotechnol* 30(4):1229–1238
- Naseem M, Philippi N, Hussain A, Wangorsch G, Ahmed N, Dandekar T (2012) Integrated systems view on networking by hormones in *Arabidopsis* immunity reveals multiple crosstalk for cytokinin. *Plant Cell* 24(5):1793–1814
- Pan X, Welti R, Wang X (2010) Quantitative analysis of major plant hormones in crude plant extracts by high-performance liquid chromatography-mass spectrometry. *Nat Protoc* 5:986–992
- Park SJ, Kim SL, Lee S, Je BI, Piao HL, Park SH, Kim CM, Ryu CH, Park SH, Xuan YH, Colasanti J, An G, Han CD (2008) Rice indeterminate 1 (OsId1) is necessary for the expression of Ehd1 (early heading date 1) regardless of photoperiod. *Plant J* 56(6):1018–1029
- Prasad B, Eizenga GC (2008) Rice sheath blight disease resistance identified in *Oryza* spp. *Accessions Plant Dis* 92(11):1503–1509
- Robert-Seilaniantz A, Grant M, Jones JD (2011) Hormone crosstalk in plant disease and defense: more than just jasmonate-salicylate antagonism. *Annu Rev Phytopathol* 49:317–343
- Savary S, Castilla NP, Elazegui FA, McLaren CG, Ynalvez MA, Teng PS (1995) Direct and indirect effects of nitrogen supply and disease source structure on rice sheath blight spread. *Phytopathology* 85(9):959–965
- Savary S, Willocquet L, Elazegui FA, Castilla NP, Teng PS (2000) Rice pest constraints in tropical asia: quantification of yield losses due to rice pests in a range of production situations. *Plant Dis* 84(3):357–369
- Seo PJ, Ryu J, Kang SK, Park CM (2011) Modulation of sugar metabolism by an INDETERMINATE DOMAIN transcription factor contributes to photoperiodic flowering in *Arabidopsis*. *Plant J* 65(3):418–429
- Shah JM, Raghupathy V, Veluthambi K (2009) Enhanced sheath blight resistance in transgenic rice expressing an endochitinase gene from *Trichoderma viridis*. *Biotechnol Lett* 31(2):239–244
- Sun Q, Li TY, Li DD, Wang ZY, Li S, Li DP, Han X, Liu JM, Xuan YH (2019) Overexpression of loose plant architecture 1 increases planting density and resistance to sheath blight disease via activation of PIN-FORMED 1a in rice. *Plant Biotechnol J* 17(5):855–857
- Volz R, Kim SK, Mi J, Mariappan KG, Siodmak A, Al-Babili S, Hirt H (2019) A chimeric IDD4 repressor constitutively induces immunity in *Arabidopsis* via the modulation of salicylic- and jasmonic acid homeostasis. *Plant Cell Physiol* 60(7):1536–1555
- Wang R, Lu L, Pan X, Hu Z, Ling F, Yan Y, Liu Y, Lin Y (2015) Functional analysis of OsPGIP1 in rice sheath blight resistance. *Plant Mol Biol* 87(1–2):81–191
- Welch D, Hassan H, Bliou I, Immink R, Heidstra R, Scheres B (2007) *Arabidopsis* JACKDAW and MAGPIE zinc finger proteins delimit asymmetric cell division and stabilize tissue boundaries by restricting SHORT-ROOT action. *Genes Dev* 21(17):2196–2204
- Wu X, Tang D, Li M, Wang K, Cheng Z (2013) Loose plant Architecture1, an INDETERMINATE DOMAIN protein involved in shoot gravitropism, regulates plant architecture in rice. *Plant Physiol* 161(1):317–329
- Xuan YH, Priatama RA, Huang J, Je BI, Liu JM, Park SJ, Piao HL, Son DY, Lee JJ, Park SH, Jung KH, Kim TH, Han CD (2013) Indeterminate domain 10 regulates ammonium-mediated gene expression in rice roots. *New Phytol* 197(3):791–804
- Yamaguchi M, Ohtani M, Mitsuda N, Kubo M, Ohme-Takagi M, Fukuda H, Demura T (2010) VND-INTERACTING2, a NAC domain transcription factor, negatively regulates xylem vessel formation in *Arabidopsis*. *Plant Cell* 22(4):1249–1263
- Yoo SD, Cho YH, Sheen J (2007) *Arabidopsis* mesophyll protoplasts: a versatile cell system for transient gene expression analysis. *Nat Protoc* 2(7):1565–1572
- Yuan P, Zhang C, Wang ZY, Zhu XF, Xuan YH (2018) RAVL1 activates brassinosteroids and ethylene signaling to modulate response to sheath blight disease in rice. *Phytopathol* 108(9):1104–1113
- Zazimalova E, Murphy AS, Yang H, Hoyerova K, Hosek P (2010) Auxin transporters—why so many? *Cold Spring Harb Perspect Biol* 2(3):a001552

Publisher's Note

Springer Nature remains neutral with regard to jurisdictional claims in published maps and institutional affiliations.

Submit your manuscript to a SpringerOpen® journal and benefit from:

- Convenient online submission
- Rigorous peer review
- Open access: articles freely available online
- High visibility within the field
- Retaining the copyright to your article

Submit your next manuscript at ► [springeropen.com](https://www.springeropen.com)